Ecotoxicology and Environmental Safety 280 (2024) 116535

Contents lists available at ScienceDirect

Ecotoxicology and Environmental Safety

journal homepage: www.elsevier.com/locate/ecoenv

Assessing sorption of fluoroquinolone antibiotics in soils from a K_d compilation based on pure organic and mineral components

Joel Fabregat-Palau [a,b,*], Anna Rigol [b,c], Peter Grathwohl [a], Miquel Vidal [b]

[a] *Department of Geosciences, University of Tübingen, Schnarrenbergstraße 94-96, Tübingen 72076, Germany*
[b] *Department of Chemical Engineering and Analytical Chemistry, University of Barcelona, Martí i Franquès 1-11, Barcelona 08028, Spain*
[c] *Institut de Recerca de l'Aigua (IdRA), Universitat de Barcelona, Martí i Franquès 1-11, Barcelona 08028, Spain*

ARTICLE INFO

Edited by Dr G Liu.

Keywords:
Fluoroquinolones
Sorption
Humic substances
Metal oxides
Phyllosilicate minerals
Soil

ABSTRACT

The presence of fluoroquinolone (FQ) antibiotics in soils may cause a threat to human health due to overexposure and the generation of antibiotic resistance genes. Understanding their sorption behavior in soils is important to predict subsequent FQ (bio) availability. Here, FQ sorption in pure soil organic (*i.e.*, humic substances) and mineral (*i.e.*, metal oxides; phyllosilicates) components is evaluated through a solid-liquid distribution coefficient (K_d (FQ)) dataset consisting of 243 entries originated from 80 different studies, to elucidate their respective contribution to the overall K_d (FQ) in bulk soils. First, different factors affecting FQ sorption and desorption in each of these soil phases are critically discussed. The strong role of pH in K_d (FQ), due to the simultaneous effect on both FQ speciation and surface charge changes, encouraged the derivation of normalized sorption coefficients for the cationic, zwitterionic and anionic FQ species in humic substances and in different phyllosilicates. K_d (FQ) in metal oxides revealed a key role of metal nature and material specific surface area due to complexation sorption mechanisms at neutral pH. Cumulative distribution functions (CDF) were applied to each dataset to establish a sorption affinity range for each phase and to derive best estimate K_d (FQ) values for those materials where normalized sorption coefficients to FQ species were unavailable. The data analysis conducted in the different soil phases set the basis for a K_d (FQ) prediction model, which combined the respective sorption affinity of each phase for FQ and phase abundance in soil to estimate K_d (FQ) in bulk soils. The model was subsequently validated with sorption data in well characterized soils compiled from the literature.

1. Introduction

Fluoroquinolones (FQ) are antimicrobial compounds used for treating human and animal diseases against both Gram-positive and Gram-negative pathogens (Van et al., 2020). They are frequently found in water bodies, posing a risk to aquatic species (Chen et al., 2016; Du et al., 2019; Ding et al., 2024). Furthermore, their use in veterinary medicine led to the presence of concentration levels around mg kg^{-1} in chicken, poultry and piggery droppings, which are often used as fertilizers in agricultural practices, leading to levels around μg kg^{-1} in agricultural soils (Riaz et al., 2018; Fang et al., 2023). Exposure to FQ in bacterial communities may lead to the generation and transfer of specific antibiotic resistance genes (Redgrave et al., 2014; Yao et al., 2020), decreasing the effectiveness of FQ to treat infections, and eventually becoming a potential threat to humans (WHO, 2017). In addition, recent findings of long-term side effects of FQ on humans led to restrictions on their prescription in the EU (EMA, 2019; Zhang et al., 2022; Shao et al., 2023).

Studying the degradation, mobility, and accumulation to soils and related dose exposure of FQ is crucial for risk assessment studies (USEPA, 2007). In terms of mobility assessment, the environmental fate of FQ is mainly controlled by their sorption to soil particles, which is pH dependent. Many of the FQ contain both a carboxyl and a piperazine functional group, with pKa_1 and pKa_2 values around 6.0 and 8.5, respectively. Thus, they can be found as cationic (+), zwitterionic (+/-) or anionic (-) species depending on the environmental conditions (Van Doorslaer et al., 2014). The simultaneous presence of different FQ species at environmentally relevant pH values complicates the derivation of accurate sorption prediction models in bulk soils (Fabregat-Palau et al., 2022), and evaluating the sorption of FQ in isolated organic and mineral soil phases may be a complementary approach to better assess their interaction in soils.

---

* Corresponding author at: Department of Geosciences, University of Tübingen, Schnarrenbergstraße 94-96, Tübingen 72076, Germany.
E-mail address: joel.fabregat-palau@uni-tuebingen.de (J. Fabregat-Palau).

https://doi.org/10.1016/j.ecoenv.2024.116535
Received 12 February 2024; Received in revised form 28 May 2024; Accepted 30 May 2024

Humic substances (HS, *i.e.,* humin, humic acid (HA) and fulvic acid (FA)) are the main contributors to the organic carbon (OC) in the soil. FQ have shown a strong tendency to bind to HS, but this process is dependent on the physicochemical properties of the substance (*i.e.,* amount and nature of functionalities), and of the aqueous solution (*i.e.,* pH, ionic strength and dissolved organic carbon (DOC) content), resulting in some disagreements on the interaction mechanisms suggested (Pan et al., 2012a; Aristilde and Sposito, 2013; Martínez-Mejía et al., 2017; Fabregat-Palau et al., 2023). Furthermore, analyses to assess sorption differences for FQ in HA and FA fractions are lacking. In regard to the mineral soil fraction, evidences of FQ-metal bindings through covalent bonds may suggest a positive role of metal oxides and hydrous oxides (*e.g.*, Fe, Al, Ti, Mn) in FQ sorption in bulk soils (Cuprys et al., 2018), but studies assessing the role of the metal in FQ sorption are scarce. Phyllosilicate minerals are also relevant in FQ sorption in soils (Leal et al., 2013; Fabregat-Palau et al., 2022), although their sorption affinity depends on the phyllosilicate nature (Wan et al., 2013) and on the physicochemical properties of the solution (Wu et al., 2010; Li et al., 2011; Chang et al., 2016; Liu et al., 2017). Nevertheless, studies rationalizing the role of phyllosilicates in FQ sorption are still lacking.

The solid-liquid distribution coefficient (K_d) is a relevant input parameter for environmental prediction models (USEPA, 2009), but K_d values for FQ are affected by multiple sources of variability. A few parametric models to predict K_d (FQ) in bulk soils based on soil properties have been suggested (Vasudevan et al., 2009; Gong et al., 2012; Fabregat-Palau et al., 2022). Alternatively, a study attempted to predict K_d for levofloxacin based on the separated cationic exchange contribution of individual organic and mineral components (Hanamoto et al., 2019), but such an approach was explored only for a limited range of pH and soils, thus not considering FQ speciation. Hence, there is still a need for a synthesis concerning the role of different soil fractions and FQ species in the overall K_d (FQ) in bulk soils.

This work aims to compile and synthesize current literature sorption and desorption data for FQ and elucidate the main properties governing their sorption in relevant soil organic and mineral fractions, to better understand the overall sorption in bulk soils. First, K_d (FQ) sorption datasets in HS, metal oxides, and phyllosilicate minerals are built. Using this information, the effect of sorbent properties (*e.g.*, pH, specific surface area (SSA)) and other experimental factors (*e.g.*, FQ concentration, ionic strength), as well as the desorption behavior and interaction mechanisms governing FQ sorption, are discussed. The contribution of each soil fractions to the overall K_d (FQ) in bulk soils is finally assessed by performing a prediction exercise based on the data derived from this investigation for each pure soil organic and mineral component.

2. Materials and methods

2.1. *Fluoroquinolones under study*

Only sorption data derived for norfloxacin (NOR), ciprofloxacin (CIP), enrofloxacin (ENR), ofloxacin (OFL) and levofloxacin (LEV) were considered, as they were the most frequent studied FQ with the most data available in the literature. Their chemical structures and main physicochemical properties are listed in Table 1, whereas the speciation profile of a representative FQ (*i.e.*, NOR) at varying pH is depicted in Fig. S1. As previous studies demonstrated that these FQ have analogous sorption in soils (Fabregat-Palau et al., 2022), in this work, their sorption data was pooled to examine the role of soil phases properties on FQ sorption. However, sorption of other FQ (*i.e.*, gatifloxacin (GAT), enofloxacin (ENO)) is also eventually discussed.

Table 1
Chemical structures and main physicochemical properties of selected fluoroquinolones.

FQ	Acronym	CAS number	Molecular Weight	Chemical structure	pKa_1 / pKa_2[a]	Solubility (g L^{-1})[b]	log D[b]
Norfloxacin	NOR	70458–96–7	319.3	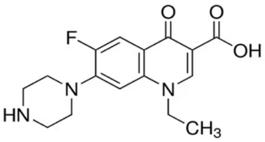	6.20 / 8.55	171 (pH 3) 1.3 (pH 7) 312 (pH 11)	-2.29 (pH 3) -1.60 (pH 7) -2.90 (pH 11)
Ciprofloxacin	CIP	85721–33–1	331.3	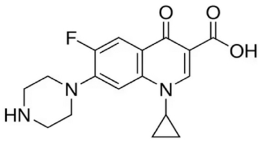	6.30 / 8.61	98 (pH 3) 1.8 (pH 7) 66 (pH 11)	-2.45 (pH 3) -1.32 (pH 7) -3.01 (pH 11)
Enrofloxacin	ENR	93106–60–6	359.4	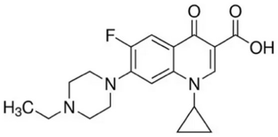	6.22 / 7.90	21 (pH 3) 0.17 (pH 7) 80 (pH 11)	-1.20 (pH 3) 0.74 (pH 7) -1.80 (pH 11)
Ofloxacin	OFL	82419–36–1	361.4	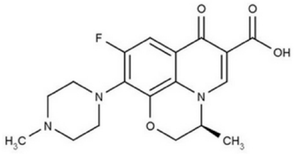	6.13 / 8.21	61 (pH 3) 0.77 (pH 7) 879 (pH 11)	-2.22 (pH 3) -1.21 (pH 7) -2.90 (pH 11)
Levofloxacin	LEV	100986–85–4	361.4	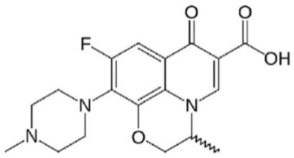	6.13 / 8.21	61 (pH 3) 0.77 (pH 7) 879 (pH 11)	-2.22 (pH 3) -1.21 (pH 7) -2.90 (pH 11)

[a] Data from Van Doorslaer et al., (2014); [b] Lipophilicity data estimated using ACD/Percepta software (www.acdlabs.com).

2.2. *Data analysis to derive fluoroquinolone solid-liquid distribution coefficients*

The solid-liquid distribution coefficient (K_d, [L kg^{-1}]), defined as the ratio between the pollutant concentration in the solid phase (C_S, [mg kg^{-1}]) and the remaining pollutant concentration in the liquid phase (C_W, [mg L^{-1}]) under equilibrium conditions, is the main sorption parameter discussed in this work. It is considered a parameter descriptive of the bulk sorption affinity within the sorbent-sorbate system (USEPA, 2009).

K_d is often derived from batch sorption experiments (OECD, 2000). However, sometimes K_d is not explicitly reported in literature studies, which require indirect approaches to derive it from other available sorption data. The criteria used in this work to derive K_d (FQ) values from literature data are detailed in Section S1. Briefly, K_d (FQ) data resulting from sorption isotherms was preferred as being the most robust sorption approach. Additionally, K_d (FQ) values were derived from sorption percentages, OC normalized sorption coefficients (K_{OC}) or fitted kinetic data. Focus was on the low FQ initial concentration (C_{in} [mg L^{-1}], generally < 25 mg L^{-1}), thus permitting us to assume that the resulting K_d data are from the linear range of sorption isotherms observed in soils (Fabregat-Palau et al., 2022). Regardless of the data used to derive K_d (FQ) entries of the datasets (see Section S1), information on other sorption parameters (*e.g.*, maximum loading capacities (Q_{MAX}) and pseudo-second order initial kinetic rate constants (V_0)) was also introduced in the compilations as additional information on the sorption process. Relevant information on the sorbent and solution physicochemical properties, as well as the experimental conditions used to derive sorption data, was also gathered as ancillary information to better inform K_d (FQ) values.

2.3. *Building-up compilations of K_d (FQ) in soil phases and soils*

2.3.1. *The case of humic substances*

Regarding K_d (FQ) compilation for HS, it only considered data for HA and FA, as sorption data in the humin fraction was not available. Ancillary data on the physicochemical properties of the HA and FA (*i.e.*, total and aromatic carbon contents) and experimental conditions were also included in the dataset. Sorption data originated from experimental approaches using solubilized organic fractions, such as dialysis (Carmosini and Lee, 2009), fluorescence quenching (Wang et al., 2015), cyclic voltammetry (Antilen et al., 2016) and affinity capillary electrophoresis (Schmitt-Kopplin et al., 1999) experiments were also accepted as they also provided quantitative information on the FQ – DOC interaction processes. Table S1 summarizes the K_d (FQ) compilation for HS, which has a total of 118 K_d (FQ) entries originated from 18 different studies. Most of the entries were directly reported from experiments at a single tested C_{in}, while 26 K_d (FQ) entries were derived from reported isotherm data and, to a lesser extent, from reported K_{OC} and kinetic data.

2.3.2. *The case of metal oxides and hydrous oxides*

The compilation of K_d (FQ) values in metal oxides and hydrous oxides originated only from batch experiments, and it also included ancillary information of sorbent physicochemical properties (*i.e.*, SSA, pH_{ZPC}) and experimental conditions. Table S2 summarizes the K_d (FQ) compilation for metal oxides and hydrous oxides, which includes data for oxides and hydrous oxides of Cu, Zn, Ni, Fe, Ti, Al, Mn, Mg and Si. Although some of these phases may be present only at trace levels in soils, their inclusion was justified to help elucidate specific sorption mechanisms. K_d (FQ) available entries were obtained mostly at a slightly acidic/neutral pH ($\approx 5 - 7$), which represents a pH range when FQ sorption in these sorbents is generally maximized (Paul et al., 2012; Najafpoor et al., 2019; Zhu et al., 2020). The total number of K_d (FQ) entries in the dataset was 57, originated from 38 different studies, with 48 K_d (FQ) entries derived from sorption isotherm data and, to a lesser extent, from sorption percentages and kinetic data.

2.3.3. *The case of phyllosilicates*

Phyllosilicate minerals can be roughly grouped as 1:1 (*e.g.*, kaolinite) and 1:2 dioctahedral minerals. Some 1:2 phyllosilicate minerals can expand their interlayer to host organic pollutants (*e.g.*, montmorillonite, hereinafter referred to as 1:2 swelling), contrary to other phyllosilicates that cannot expand (*e.g.*, illite, hereinafter referred as 1:2 non-swelling). Compilation of K_d (FQ) values for phyllosilicate minerals originated only from batch experiments and both 1:1 and 1:2 dioctahedral phyllosilicates. Ancillary information on clay properties (*i.e.*, cation exchange capacity (CEC), SSA) and experimental conditions was also compiled. Table S3 summarizes the K_d (FQ) compilation for phyllosilicates. They were grouped as 1:2 swelling (*i.e.,* rectorite, montmorillonite), 1:2 non-swelling (*i.e.,* sepiolite, palygorksyte, illite, and vermiculite), and 1:1 phyllosilicates (*i.e.,* kaolinite). The dataset consisted in a total of 68 K_d (FQ) entries originated from 30 different studies, of which 57 were derived from reported isotherm data.

2.3.4. *The case of bulk soils*

To evaluate the individual contributions of organic and mineral soil components in the overall K_d (FQ) in bulk soils, a subset of soils that fulfilled the following accepting criteria were selected from the literature: 1) to report sorption isotherm data for at least one of the FQ under study in this work (*i.e.*, NOR, CIP, ENR, OFL); 2) to report soil properties, such as pH, organic matter content and mineralogical information. The total number of soils that fulfilled these criteria was 46, originated from seven different studies, leading to a total of 68 K_d (FQ) entries. Information on the selected soils is provided in Table S4.

3. Results and discussion

3.1. *Sorption behavior of FQ in humic substances*

3.1.1. *Sorption kinetics of FQ in humic substances*

Kinetic data of FQ in HS are only available for HA and reveal fast sorption during the initial stages of the reaction, followed by a slower uptake until reaching equilibrium (Pan et al., 2012b). Generally, 48 hours are enough to achieve the sorption equilibrium regardless of tested FQ and experimental conditions (Zhang et al., 2012; Martínez-Mejía et al., 2017; Fabregat-Palau et al., 2023), which agrees with kinetic observations in organic soils (Conkle et al., 2010). The kinetic data are generally well-fitted by the pseudo-second order model (PSOM) equation (Blanchard et al., 1984). V_0 values, a parameter that indicates how fast the pollutant kinetic uptake is in the first stage of the sorption process, vary within two orders of magnitude (*i.e.*, 7 – 300 mg g^{-1} h^{-1}, see Table S1).

3.1.2. *Comparison between humic and fulvic acid fractions*

Previous research conducted under controlled laboratory conditions suggests slightly lower FQ sorption in FA than in HA fractions (Carmosini and Lee, 2009; Aristilde and Sposito, 2013). To better assess the FQ sorption differences within HS fractions, K_d (FQ) populations for HA and FA summarized in Table S1 were compared in a box plot after confirming the absence of outliers using Grubb's test ($\alpha = 0.05$). As pH is expected to play a role in sorption in HS (see Section 3.1.4), K_d (FQ) data was restricted to those entries within a pH range of 4 – 8, as K_d (FQ) data for FA were unavailable at other pH values. Results are shown in Fig. S2, and a t-test ($\alpha = 0.05$) revealed statistically comparable K_d (FQ) populations for both HA and FA fractions. Hence, K_d (FQ) data for FA and HA were pooled to examine the role of HS in FQ sorption in following statistical analyses.

3.1.3. *Sorption isotherms of FQ in humic substances*

Sorption isotherms for FQ in HA and FA are typically non-linear and well-fitted by either the Freundlich or the Langmuir models (Carmosini and Lee, 2009; Zhang et al., 2012; Martínez-Mejía et al., 2017; Zhu et al., 2018; Zhao et al., 2019; Fabregat-Palau et al., 2023), and to other non-linear models (Antilen et al., 2016; Wang et al., 2017), although linear or close-to-linear sorption isotherms have also been observed (Aristilde and Sposito, 2013). At low initial concentrations, FQ molecules are sorbed at highly-affinity sorption sites, whereas at higher concentrations, sorption at sites with lower FQ affinity takes place, eventually reaching saturation of HS sites. K_d (FQ) and Q_{MAX} (FQ) values in Table S1 range 100 – 871,000 L kg^{-1} and 40 – 530 mg g^{-1}, respectively, depending on the physicochemical properties of both solid and liquid phases, with median values of 23,600 L kg^{-1} and 110 mg g^{-1}. According to the generally high K_d (FQ) and Q_{MAX} (FQ) values reported, a high sorption of FQ in organic soils (with large amounts of HS) can be anticipated.

3.1.4. Effect of pH in FQ sorption in humic substances

K_d (FQ) in HA shows a bell-shaped dependence with pH, with maximum sorption at pH ~ 5 – 6 (Lützhøft et al., 2000; Zhang et al., 2012; Fabregat-Palau et al., 2023), thus indicating that sorption of the positively charged FQ species (*i.e.*, cationic and zwitterionic) is favored. At acidic conditions, the protonated FQ species may interact with HA through cation exchange and cation-π mechanisms with HS deprotonated and aromatic functionalities, respectively (Martínez-Mejía et al., 2017; Zhao et al., 2017). Additionally, according to computational studies, HA are expected to undergo structural changes, *e.g.*, rearrange their hydrophobic and hydrophilic regions, disrupting intramolecular hydrogen bonding to facilitate intermolecular hydrogen bonding with FQ (Aristilde and Sposito, 2010). The hydrogen bond interaction between FQ and HA has also been confirmed by Fourier-transformed infrared (FTIR) spectroscopic observations at acidic to neutral pH (Zhang et al., 2012; Liu et al., 2017; Zhu et al., 2018). At neutral conditions, a higher number of functionalities of the FQ are deprotonated. Therefore, the positive charge of the zwitterionic FQ form can better interact through electrostatic interactions, although the negative charge of the carboxylate group leads to higher repulsions with these functionalities. These repulsions gain relevance at pH > pKa$_2$ when the anionic FQ form is predominant. Both hydrophobic and π-π interactions are not expected to be highly affected by pH changes, which may explain the low sorption of FQ in HA at basic pH conditions (Zhao et al., 2019).

To better elucidate the effect of pH changes on FQ sorption in HS, a pH-distribution model (Equation 1), which has been used to derive normalized sorption coefficients for ionizable species (Teixidó et al., 2011), was used to derive normalized sorption coefficients for each FQ species as:

$$\log K_d^{pH(FQ)} = \log K_d^{+} f(FQ^{+}) + \log K_d^{\pm} f(FQ^{\pm}) + \log K_d^{-} f(FQ^{-}) \tag{1}$$

where *f(FQ$^+$)*, *f(FQ$^\pm$)* and *f(FQ$^-$)* are the fractions of each cationic, zwitterionic and anionic FQ species at a given pH value, respectively, calculated using the mean pKa$_1$ and pKa$_2$ values (*i.e.*, 6.2 and 8.3, respectively) of all examined FQ as shown in Eqs. 2 – 4 (Septian et al., 2018):

$$f(FQ^{+}) = \frac{1}{1 + 10^{(pH - pK_{a1})} + 10^{(2pH - pK_{a1} - pK_{a2})}} \tag{2}$$

$$f(FQ^{\pm}) = \frac{1}{1 + 10^{(pK_{a1} - pH)} + 10^{(pH - pK_{a2})}} \tag{3}$$

$$f(FQ^{-}) = \frac{1}{1 + 10^{(pK_{a2} - pH)} + 10^{(pK_{a1} + pK_{a2} - 2pH)}} \tag{4}$$

Equation 1 was used to fit the K_d (FQ) data of our HS compilation within a pH range of 3 – 11 (see Fig. 1). This resulted in a significant ($r^2 = 0.47$; n = 118; $p < 0.05$) fit, with the log K_d values of species coefficients listed in Table 2. The sequence of sorption affinity was FQ$^\pm$ > FQ$^+$ >> FQ$^-$, which confirmed the lower sorption affinity of negatively charged species in HA and the key role of FQ speciation in the overall sorption process. Nevertheless, it is observed that Equation 1 is unable to explain electrostatic repulsions at extreme pH values, where a certain FQ species predominates, but HS surface charge is still affected by pH changes. A second-order polynomial equation has been successfully used to model the bell-shaped K_d (FQ) dependence in HA elsewhere (Fabregat-Palau et al., 2023), with this model being able to account for electrostatic repulsions at extreme pH values. Accordingly, the overall K_d (FQ) data in Table S1 was then fit to a second-order polynomial equation over the pH range of 3 – 11 (see Fig. 1), resulting in a significant ($r^2 = 0.46$; n = 118; $p < 0.05$) correlation with the form of $\log K_d = -0.09\ (\pm 0.02)\ pH^2 + 1.02\ (\pm 0.31)\ pH + 1.79\ (\pm 0.98)$ and a maximum log K_d (FQ) value of 5.81 occurring at pH ~ 5.7.

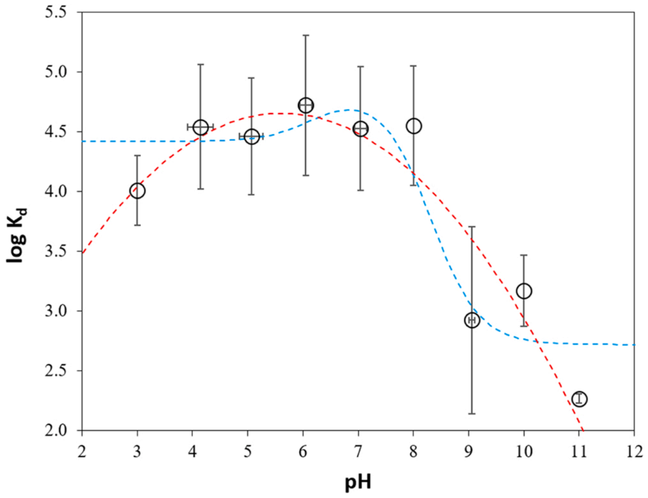

Fig. 1. Relationship between log K_d values and pH for the overall K_d (FQ) dataset in humic substances. Blue dashed line: pH-distribution model (Equation 1); Red dashed line: second order polynomic model; Mean log K_d and pH values were grouped within ± 1 pH units to facilitate data visualization, although the resulting fitting considered the individual log K_d values; bars indicate standard deviations.

Table 2
Fitting parameters of the pH-distribution model for each examined phase type. 95 % confidence intervals of the fitted parameters are given.

Soil phase	N	log K_d (FQ$^+$)	log K_d (FQ$^\pm$)	log K_d (FQ$^-$)	r^2
Humic substances	118	4.42 ± 0.16	4.81 ± 0.22	2.73 ± 0.33	0.47
1:1 phyllosilicates	21	3.36 ± 0.39	3.09 ± 0.40	1.83 ± 0.71	0.48
1:2 non-swelling phyllosilicates	13	3.72 ± 0.40	3.35 ± 0.56	2.49 ± 0.68	0.55
1:2 swelling phyllosilicates	34	5.00 ± 0.40	5.04 ± 0.53	3.34 ± 0.59	0.45

3.1.5. Effect of ionic strength and ion composition in FQ sorption in humic substances

FQ sorption in HA and FA decreases gradually when increasing the concentration of cations (*i.e.*, calcium, magnesium, and potassium), although the extent of this effect depends on the chemical properties of the HA (Carmosini and Lee, 2009; Pan et al., 2012a; Zhang et al., 2012; Martínez-Mejía et al., 2017; Fabregat-Palau et al., 2023). This agrees with electrostatic and cation exchange interactions being suggested to play a role in FQ sorption after observing shifts in FTIR bands attributed to the protonated piperizine group of the FQ (Zhang et al., 2012). Therefore, higher cation concentrations in solution can better compete for exchangeable sites and thus decrease FQ sorption. FTIR and ^{13}C nuclear magnetic resonance (NMR) data also identified aromatic regions of the HA as responsible for electron donor-acceptor π-π interactions (Zhang et al., 2012; Zhao et al., 2019), these have been found to be of lesser relevance than cation-π interactions at acidic to neutral pH in highly aromatic materials (Zhao et al., 2017), thus reinforcing the competitive role of cations in FQ sorption. For several cations, as for Cu, which can coexist with FQ in polluted agricultural soils, the formation of ternary complexes is suggested (Pan et al., 2012a; Zhao et al., 2019) which appear to depend on the ionic potential (valence/ionic radius) of the metal and the chemical functionalities of the HA (Aristilde and Sposito, 2008).

3.1.6. *Desorption of FQ from humic substances*

Desorption data for FQ in HS are scarce and only available for HA. Desorption kinetics of FQ in HA show time scales of $\leq$ 48 hours to reach desorption equilibrium (Martínez-Mejía et al., 2017), and desorption isotherms often show a non-linear pattern and have usually been fitted to the Freundlich model (Martínez-Mejía et al., 2017; Fabregat-Palau et al., 2023), indicating that those molecules sorbed in low affinity sites are prone to being remobilized into water. Reported desorption percentages in a single batch desorption cycle ranged 18 – 20 % when conducting desorption experiments immediately after sorption (Martínez-Mejía et al., 2017), whereas lower values (ranging 2.7 – 9.3 %) were obtained when sorption residues were submitted to conditions simulating soil ageing (Fabregat-Palau et al., 2023). Desorption K_d values ($K_{d,des}$) derived within the linear range of the desorption isotherms for a single desorption cycle are higher than the respective sorption K_d, proving that a significant fraction of FQ is irreversibly sorbed (Martínez-Mejía et al., 2017; Fabregat-Palau et al., 2023).

3.2. *Sorption behavior of FQ in metal oxides and hydrous oxides*

3.2.1. *Sorption kinetics of FQ in metal oxides and hydrous oxides*

Sorption kinetics of FQ in different metal oxides and hydrous oxides have been evaluated (*e.g.*, Fe_3O_4 (Moradi et al., 2016), FeO(OH) (Zhang and Huang, 2007), Al_2O_3 (Najafpoor et al., 2019), TiO_2 (Gan et al., 2018)) and revealed time scales of $\leq$ 48 hours to reach sorption equilibrium regardless the evaluated metal, FQ and experimental conditions tested, with V_0 values generally ranging 9 – 110 mg g^{-1} h^{-1} (see Table S2).

3.2.2. *Sorption isotherms of FQ in metal oxides and hydrous oxides*

Sorption isotherms for FQ in metal oxides and hydrous oxides at neutral pH reveal different patterns. Regarding Al and Fe, derived K_d (FQ) values from Freundlich ($1/n < 1$) and Langmuir fittings ranged 80 – 1100 L kg^{-1} and 80 – 5000 L kg^{-1}, respectively, with median K_d (FQ) values of around 550 L kg^{-1} (Gu and Karthikeyan, 2005; Lorphensri et al., 2006; Zhang and Huang, 2007; Tan et al., 2015). Other non-linear isotherm fittings such as the Langmuir-Freundlich (Goyne et al., 2005), Temkin (Moradi et al., 2016; Najafpoor et al., 2019) and Freundlich ($1/n > 1$, Fries et al., 2016) have also been observed for Al and Ti oxides. Quartz sand, mainly composed of SiO_2, has low K_d (FQ) values (ranging 1 – 15 L kg^{-1}, with a median of 8.7 L kg^{-1}) and Q_{MAX} (FQ) values (ranging 0.005 – 0.022 mg g^{-1}, with a median of 0.019 mg g^{-1}). Contrarily, Fe and Al oxides and hydrous oxides show higher Q_{MAX} (FQ) values, ranging 2 – 165 mg g^{-1} with a median Q_{MAX} (FQ) value of 18 mg g^{-1}. These Q_{MAX} (FQ) values are generally lower than those reported for HA despite the generally larger SSA of metal oxides (the SSA of HA is in the range of 5 – 40 m^2 g^{-1} (Wang et al., 2015; Liu et al., 2017), whereas SSA for metals is often within the 10^1 – 10^3 m^2 g^{-1} range), which suggests that metal oxides and hydrous oxides contain a lower number of interaction sites per square meter of mineral surface able to bind FQ compared to the soil organic fractions.

3.2.3. *Effect of pH in FQ sorption in metal oxides and hydrous oxides*

The effect of pH on FQ sorption in metal oxides and hydrous oxides has been widely evaluated in the literature (Gu and Karthikeyan, 2005; Lorphensri et al., 2006; Paul et al., 2012; 2014; Rakshit et al., 2013), revealing a bell-shaped K_d (FQ) *vs.* pH pattern, with maximum sorption often within the pH 6 – 7 range, where the FQ zwitterionic species are predominant. Besides pH, pH_{ZPC} may play a major role in sorption, as the mineral surface bears an overall positive charge at $pH < pH_{ZPC}$ and a negative charge at $pH > pH_{ZPC}$. At $pH < pKa_{1,}$ electrostatic repulsion occurs between the positively charged FQ and mineral surface, and FQ sorption is unfavoured, although the reduced sorption observed could be explained by goethite-induced deprotonation of the FQ carboxylate moiety at $pH < pKa_1$ (Trivedi and Vasudevan, 2007). At $pKa_1 > pH$, complexation mechanisms become predominant. Sorption in these scenarios is favoured at $pH < pH_{ZPC}$, for which electrostatic interactions between the negative charge in FQ zwitterion species and the positively charged oxide surface may further contribute to sorption. At $pH > pKa_2$ and/or $pH > pH_{ZPC}$, increasing electrostatic repulsions leads to an abrupt decrease in sorption. This pattern has been observed for oxides such as FeO(OH) (Gu and Karthikeyan, 2005; Trivedi and Vasudevan, 2007; Qin et al., 2014) and Fe_3O_4 (Rakshit et al., 2013), both with maximum FQ sorption at around $pH \approx 6.0$, Al_2O_3 (maximum sorption at $pH \approx 7.0$; Lorphensri et al., 2006; Najafpoor et al., 2019) and AlO(OH) (maximum sorption at $pH \approx 7.8$; Gu and Karthikeyan, 2005). Unfortunately, the lack of reported quantitative sorption data for different metal oxides under pH conditions where cationic and anionic FQ species are predominant prevented the application of Equation 1 to estimate K_d (FQ) values based on normalized sorption coefficients of each FQ species.

3.2.4. *Effect of ionic strength and ion composition in FQ sorption in metal oxides and hydrous oxides*

Ionic strength and cationic composition of the aqueous solution also affect FQ sorption in metal oxides (Paul et al., 2012; 2014; Qin et al., 2014; Tan et al., 2015). Whereas some authors found that the presence of Ca cations enhanced FQ sorption through ternary complexes assisted by cation bridging mechanisms (Tan et al., 2015), other authors reported that the presence of Ca decreased FQ sorption due to the formation of soluble Ca-FQ complexes in solution (Qin et al., 2014). The potential effect of the presence of Na has also been examined, with inconclusive results. Although some authors reported a negligible effect of increasing Na concentration on FQ sorption in FeO(OH) at neutral pH (Gu and Karthikeyan, 2005), other authors found slight sorption enhancement of FQ in Fe_3O_4 and FeO(OH) at acidic pH with increasing Na concentration (Paul et al., 2014; Rakshit et al., 2013). These small sorption differences could be attributed to the different pH values at which the effect of Na was tested. Na cations could affect FQ sorption only at acidic pH, where high Na concentrations may better shield electrostatic repulsions between the cationic FQ species and the positively charged surface at $pH < pH_{ZPC}$. The role of soluble anions on FQ sorption in metal oxides has also been examined (Paul et al., 2012; 2014). The increasing ability of some anions to form $FQ^+ X^-$ ion pairs may lead to a reduction of electrostatic repulsions between the positively charged FQ moiety and the positively charged mineral surface at $pH < pH_{ZPC}$.

3.2.5. *Effect of metal nature and SSA in FQ sorption in metal oxides and hydrous oxides*

Computational studies have suggested that FQ are able to bind metallic atoms through covalent bonds by forming FQ-metal complexes through the carboxylate moiety of the FQ (Aristilde and Sposito, 2008). FQ-metal complex stability is more influenced by metal nature than by FQ nature for a given stoichiometry (Cuprys et al., 2018). Specifically for Fe oxides, FQ may bind to Fe atoms through monodentate, bidentate chelate, bridging binuclear bidentate and tridentate chelate complexes (Trivedi and Vasudevan, 2007; Paul et al., 2014; Qin et al., 2014), and the complexation ability may differ with the stoichiometric Fe(II)/Fe(III) ratio (Cheng and Hanna, 2018). According to FTIR data, an inner-sphere mononuclear bidentate chelate complex between an oxygen atom of both the carboxylate and carbonyl moieties of the FQ species and the metallic atoms present in the mineral surface has been suggested for goethite and hematite (Trivedi and Vasudevan, 2007; Martin et al., 2015). Differently, a bridging binuclear bidentate complex was hypothesized for magnetite, likely due to mineralogical differences among metal oxides (Rakshit et al., 2013). Moreover, inner-sphere tridentate chelates complexes were hypothesized to occur at specific crystallographic faces of goethite, although these might shift to bidentate complexes under high FQ concentration due to steric effects (Paul et al., 2014). Outer-sphere complexes have also been suggested for GAT in goethite (Li and Bi, 2019), and, at basic pH, for ENO in ferrihydrite (Wang et al., 2022). Overall, all crystallographic features of the Fe-mineral (*i.e.*, abundance of specific crystallographic phases, site density and Fe(II)/Fe(III) ratio) as well as the tested pH, FQ nature and concentration, may affect the resulting FQ – Fe complexes. Regarding other metal oxides, evidences of FQ – metal complexes through the formation of covalent bonds has also been reported for Al and Ti (Goyne et al., 2005; Paul et al., 2012).

To better evaluate the role of metal in FQ sorption, data analysis was carried out in this study mostly within a 5 – 7 pH range to reduce data variability due to pH changes, and K_d values were normalized according to the metal oxide SSA ($K_{d,SSA}$, mL m^{-2}) to exclude this additional source of variability. Table 3 summarizes the $K_{d,SSA}$ (FQ) range values calculated for metal oxides and hydrous oxides, although in some cases (*e.g.*, Cu, Zn, Ni oxides), a few sorption data were available. $K_{d,SSA}$ values followed the sequence: Cu > Zn ≥ Ni > Fe > Ti > Al > Mn ≈ Mg > Si, which roughly agrees with the Irving – Williams series describing the complexation stability of organic ligands by metallic atoms (Irving and Williams, 1953). This suggests an increasing binding affinity of FQ under neutral conditions with specific metallic atoms due to the formation of FQ – metal complexes.

To evaluate the effect of SSA, as the metal nature plays a role in the binding strength, only those entries referring to Fe hydrous oxides (*i.e.*, goethite) were considered, as being the material with the highest number of available sorption data. The pH of these data range 5 – 7, thus anticipating a minor effect of pH in this K_d (FQ) dataset. As shown in Table S2, SSA values of Fe hydrous oxides range 10 – 330 m^2 g^{-1}, suggesting that differences in K_d (FQ) values could be attributed to changes in specific surface properties. A significant linear relationship ($n = 13$; $p < 0.001$) between log K_d and log SSA was found, which described 79 % of the K_d (FQ) variability (Fig. S3). This positive relationship, with a slope statistically equal to one, confirmed the key role of SSA in the sorption of FQ in Fe hydrous oxides. As the expected SSA value for naturally occurring Fe-minerals in soils is around 10 m^2 g^{-1} (Jacobson and Fan, 2019), low K_d (FQ) value (~ 100 L kg^{-1}) can be expected.

3.2.6. Desorption of FQ from metal oxides and hydrous oxides

Desorption data for FQ in metal oxides and hydrous oxides are scarce. Available data indicate a fast kinetic desorption, reaching desorption equilibrium at very early times (Zhang and Huang, 2007). Desorption isotherms for GAT show a Freundlich-like behavior in both hematite and goethite (Li and Bi, 2019). Besides, sorption hysteresis evaluated at a single desorption cycle indicates a generally irreversible process (Goyne et al., 2005; Zhang and Huang, 2007; Tan et al., 2015), although desorption rates increase when increasing pH (Rakshit et al., 2013) and with increasing number of desorption cycles (Li and Bi, 2019).

Table 3
$K_{d,SSA}$ median and range values derived for different FQ in metal oxides and hydrous oxides.

Metal[a]	$K_{d,SSA}$ (mL m^{-2}) range	$K_{d,SSA}$ (mL m^{-2}) median	Number of entries (materials; studies)
Si	0.20	0.20	2 (2; 2)
Mn	0.74 – 1.4	0.98	4 (1; 1)
Mg	0.22 – 2.6	1.1	3 (3; 2)
Al	1.1 – 3.3	2.4	4 (4; 3)
Ti	3.6 – 39	5.9	6 (6; 6)
Fe	3.8 – 38	12	28 (23; 18)
Ni	47	47	1 (1; 1)
Zn	54	54	1 (1; 1)
Cu	176	176	1 (1; 1)

[a] Metal atom are referring to the respective oxide species (*i.e.*, SiO_2, MnO_2, MgO, TiO_2, NiO, ZnO, CuO), except for Fe and Al that included in addition hydrous oxides (*i.e.*, Fe_2O_3, Fe_3O_4, FeO(OH), Al_2O_3, AlO(OH))

3.3. Sorption of FQ in phyllosilicate minerals

3.3.1. Sorption kinetics of FQ in phyllosilicate minerals

Kinetic data of FQ in phyllosilicates revealed fast sorption in the first stage of the sorption process, followed by a slower uptake until reaching equilibrium at ≤ 24 hours regardless of the experimental conditions tested (Li et al., 2011; Liu et al., 2017; Pan et al., 2012b; Wan et al., 2013; Wang et al., 2011), which agree with kinetic observations in clay soils (Peruchi et al., 2015). Derived V_0 values vary within four orders of magnitude (range 15 – 486,000 mg g^{-1} h^{-1}, see Table S3), with higher values noted for materials with larger SSA. In general, V_0 values in phyllosilicates are higher than those derived in HS, and except for 1:2 swelling phyllosilicates, similar to those observed for metal oxides and hydrous oxides, although it is noted that V_0 values for a given FQ – clay pair may decrease at increasing pH (Roca et al., 2015).

3.3.2. Sorption isotherms of FQ in phyllosilicate minerals

Sorption isotherms for FQ in phyllosilicates are commonly fitted to the Langmuir model, although Freundlich and linear fittings have also been described (Li et al., 2011; Pei et al., 2011; Wan et al., 2013; Wang et al., 2011; Yan et al., 2012). In addition to the specific FQ – clay interactions, the selected experimental conditions appear to affect the isotherm pattern. Langmuir-pattern isotherms have been described for montmorillonite when high initial FQ concentrations (> 500 mg L^{-1}) were assessed (Wu et al., 2012a; Wan et al., 2013; Wang et al., 2011; Rivagli et al., 2014). Contrarily, Freundlich and linear isotherms were found at lower (< 77 mg L^{-1}) concentrations (Pei et al., 2011; 2022). Different-shaped isotherms (*i.e.*, Langmuir-, Freundlich- and linear-type) have been reported in montmorillonite depending on the tested pH (within the 3 – 10 range) (Roca et al., 2015). Changes in solution pH can affect both the charge properties of the clay surface and the FQ species participating in sorption, which may affect the resulting sorption isotherm pattern.

K_d (FQ) values in phyllosilicates vary within several orders of magnitude (45 – 6,600 L kg^{-1} for 1:1 phyllosilicates, with a median of 1,160 L kg^{-1}; 180 – 22,400 L kg^{-1} for 1:2 non-swelling phyllosilicates, with a median of 5,000 L kg^{-1}; and 400 – 955,000 L kg^{-1} for 1:2 swelling phyllosilicates, with a median of 50,700 L kg^{-1}) (see Table S3). Q_{MAX} (FQ) also depended on the type of phyllosilicate: for 1:1 phyllosilicates, Q_{MAX} (FQ) ranged 3 – 31 mg g^{-1}; 33 – 112 mg g^{-1} for 1:2 non-swelling; and 135 – 400 mg g^{-1} for 1:2 swelling phyllosilicates. The increasing K_d (FQ) and Q_{MAX} (FQ) sequences (1:1 < 1:2 non-swelling < 1:2 swelling phyllosilicates) agree with findings of FQ higher sorption in montmorillonite-rich soils than kaolinite-rich soils (Nowara et al., 1997). The higher sorption in 1:2 compared to 1:1 phyllosilicates might be attributed to their generally higher CEC and SSA, with enhanced sorption in swelling clays due to the extra sites able to host FQ present in the interlayer space (Okaikue-Woodi et al., 2018).

3.3.3. Effect of pH and clay nature in FQ sorption in phyllosilicate minerals

Sorption of FQ in phyllosilicate minerals is pH-dependent and expected to differ among clays (Wan et al., 2013). The pH$_{ZPC}$ of phyllosilicates is typically around 2 – 4 (Pan et al., 2012b), which suggests that they bear an overall negative surface charge under most environmental conditions. At pH < pKa$_1$, the cationic FQ species sorb at the clay surface via cationic exchange mechanisms, as proved after monitoring the desorbed cations from clay surfaces along FQ uptake (Li et al., 2011). At pH > pKa$_1$, despite the fact that FQ molecules still participate in cation exchange, sorption decreases due to increasing electrostatic repulsions with the negatively charged clay surface, being these repulsions maximized at pH > pKa_2 (Wan et al., 2013). Due to the varying surface charge properties of different phyllosilicates, and the ability of some of them to host FQ in the interlayer space, further explorations of K_d (FQ) populations in Table S3 were assessed for different pH ranges and phyllosilicates.

K_d (FQ) values from the clay compilation were grouped according to phyllosilicate type and pH (*i.e.*, pH < pKa_1, pKa_1 < pH < pKa_2, and pH > pKa_2), and statistical differences were tested among groups by means of Fisher Least Significance Differences (FLSD) tests (see Fig. S4). Despite the generally higher FQ sorption observed in 1:2 non-swelling than 1:1 phyllosilicates, statistical analysis revealed no significant differences between the literature-compiled K_d (FQ) data populations in these two clay types for any pH group (and, thus, for any FQ species). Contrarily, K_d (FQ) for 1:2 swelling phyllosilicates was generally the highest regardless of the FQ species. Moreover, sorption of cationic and zwitterion FQ species was statistically comparable in all clay types, being higher than that observed for the anionic FQ species, confirming the lowest sorption of FQ in clay minerals at basic pH (Wan et al., 2013; Li et al., 2017).

The relative sorption affinity for each FQ species was further confirmed after applying a pH-distribution model, previously used to fit K_d (FQ) HS data (Equation 1), to the K_d (FQ) data for each clay type (see Fig. 2). The model led to a significant fit ($p < 0.05$) along the different pH ranges for each clay type, and it allowed us to derive log K_d values normalized to each fraction of the cationic, zwitterionic and anionic FQ species (see Table 2). The pH-distribution model explained around 50 % of the K_d (FQ) data variance for 1:1, 1:2 non-swelling and 1:2 swelling phyllosilicates, respectively, highlighting the importance of pH in FQ sorption in phyllosilicates by modifying both FQ speciation and clay surface charge properties. Unlike for HA and FA, the application of a second-order polynomial fitting failed to describe the log K_d *vs.* pH pattern for phyllosilicates because strong decreases in K_d (FQ) were not observed at very low pH. This may be attributed to the lower pH_{ZPC} of phyllosilicates compared to that of HS ($pH_{ZPC} \sim 9$, Singaraj et al., 2019), which minimizes electrostatic repulsions between cationic FQ species and positively charged clay surfaces at extreme pH values, thus decreasing the fitting performance of second-order models and improving instead the performance of the pH-distribution model.

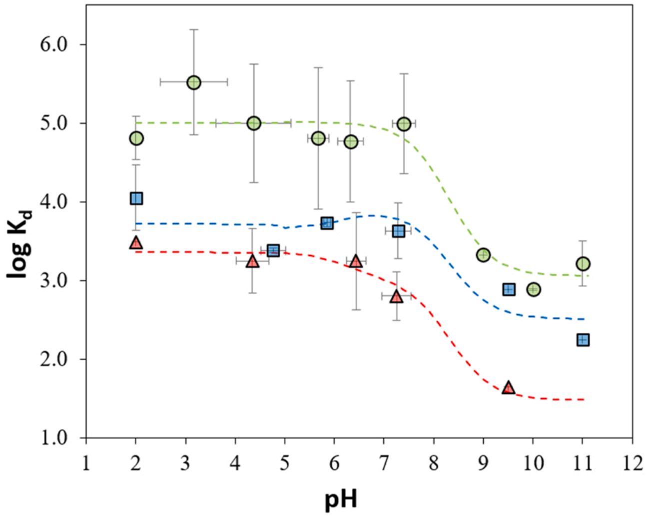

Fig. 2. Relationship between log K_d values and pH for the overall K_d (FQ) data in each phyllosilicate type reported in Table S3 (Δ: 1:1 phyllosilicates, red; □: 1:2 non-swelling phyllosilicates, blue; ○: 1:2 swelling phyllosilicates, green). Colored dashed line indicates the fitting of Equation 1 for each clay type. In all cases, mean log K_d and pH values are grouped within ± 1 pH units to facilitate data visualization, although fitting involved all individual log K_d values; bars indicate standard deviations of the original data.

3.3.4. *Effect of ionic strength in FQ sorption in phyllosilicate minerals*

As similarly seen for HA and FA, solution ionic strength and cationic composition affect the sorption of FQ in phyllosilicates due to competition for exchangeable sites. Cation exchange mechanisms are favoured for those cations with a higher charge-to-size ratio. Thus, the increase in Na levels in solution lowered FQ sorption in kaolinite (Li et al., 2017), and a greater decrease was observed for divalent cations such as Ca (Rivagli et al., 2014). Sorption of FQ in homoionic montmorillonite decreased when increasing the charge of the competitive cation saturating the clay (Na > Ca > Al, Wu et al., 2012b), excepting when Cs was the saturating cation, due to the stability of Cs – clay complexes that inhibited the exchange with positively charged FQ molecules (Yan et al., 2012). For a few cationic elements, their possible competitive role with FQ for exchange sites is affected by pH and by other concurrent equilibrium. This is the case of Cu, which may suppress FQ sorption at acidic pH (Liu et al., 2017), but instead may enhance FQ sorption at neutral to basic pH (Li et al., 2017; Pei et al., 2010). At acid pH, Cu may form soluble FQ – M complexes and then decrease FQ sorption (see Section 4.2.5), whereas at higher pH, the precipitation of $Cu(FQ)_2$ and the formation of clay–Cu–FQ ternary complexes are favoured (Pei et al., 2010; 2011; Li et al., 2017; Cuprys et al., 2018).

3.3.5. *Desorption of FQ from phyllosilicate minerals*

Contrarily to observations in HA and metal oxides, desorption data of FQ from phyllosilicates reveal almost instantaneous desorption equilibrium regardless of the initial FQ concentration and experimental conditions tested (Lv et al., 2013; Wu et al., 2012a). Desorption percentages for FQ in kaolinite and montmorillonite after a single desorption cycle were as low as 0.2 % in the presence of 10 mM $CaCl_2$, indicating a strong sorption irreversibility (Nowara et al., 1997), and ≤ 8 % under Milli-Q water conditions after five consecutive desorption cycles (Wu et al., 2012a). Desorption yields increased when increasing cation content in solution, following the trend Al > Ca > Na (Wu et al., 2012a), likely due to the higher affinity of Al for exchangeable sites, which promoted FQ desorption through cation exchange. Moreover, desorption yields increased in the presence of DOC (Li et al., 2019) and at increasing pH, likely due to increasing electrostatic repulsions at increasing pH (Wu et al., 2012a).

4. Assessment of the role of each soil component in bulk soils

4.1. *Comparison of K_d (FQ) data populations of soil components*

K_d (FQ) data populations of the soil components were analyzed in terms of cumulative distribution functions (CDF) and statistically compared among each other by means of FLSD tests, as similarly described elsewhere (Fabregat-Palau et al., 2022; Ramírez-Guinart et al., 2022), to better rank the sorption affinity of each investigated soil phase. Additional information on the CDF construction is provided in Section S2. As the metal nature plays a role in FQ sorption, the dataset for metal oxides and hydrous oxides was restricted only to Si and Fe oxides and hydrous oxides, as they are the most abundant species in soils. The dataset for clay minerals was split into those entries representative of 1:1, 1:2 non-swelling and 1:2 swelling phyllosilicates given their differing sorption capacities (see Section 3.3.3). As K_d (FQ) in some of the soil phases examined is affected by pH changes (see Section 3.1.4 and Section 3.3.3), care was taken to ensure that the proportion of entries at varying pH was similar among the different populations compared (see Fig. S5).

Fig. 3 summarizes the CDF of the K_d (FQ) populations of the soil phases and related statistical parameters (*i.e.*, geometric mean derived from the 50th percentile; geometric standard deviation to describe population variability; 5th and 95th percentiles). SiO_2 had the lowest geometric mean K_d (FQ) ($\sim$ 7 L kg^{-1}), indicating a weak sorption

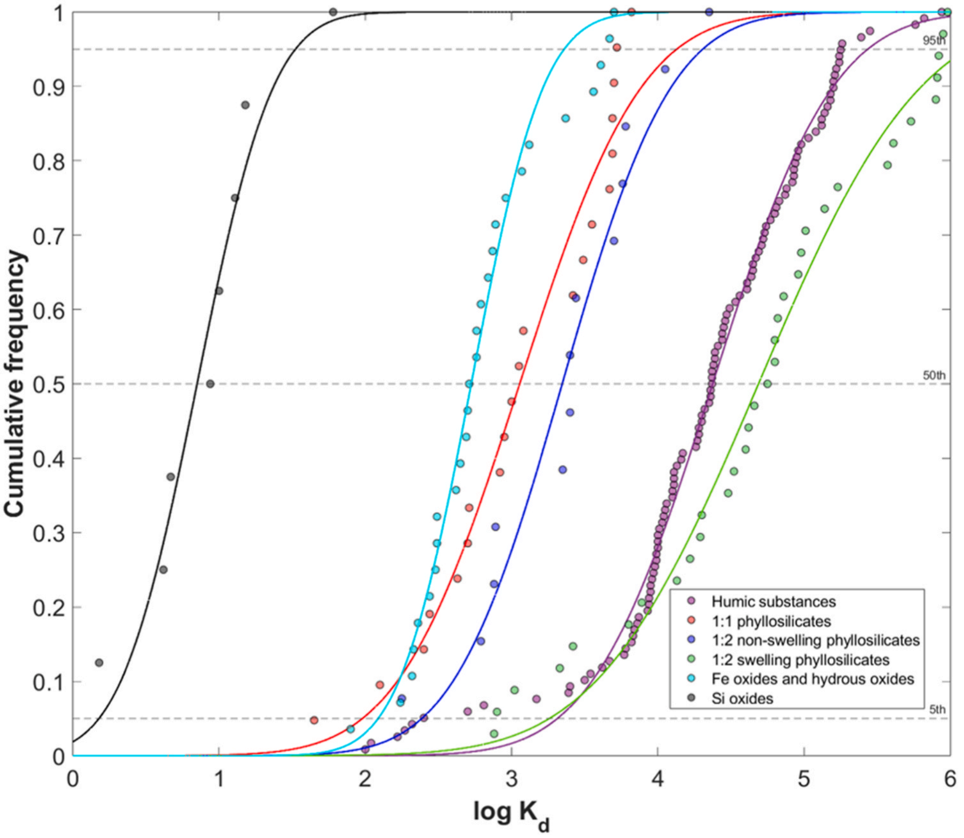

Dataset	N	GM	GSD	5th	95th	FLSD
Humic substances	118	23,530	4.5	2,007	275,850	A
1:2 swelling phyllosilicates	34	48,780	7.4	1,816	1,310,500	A
1:2 non-swelling phyllosilicates	13	2,220	3.8	243	20,246	B
1:1 phyllosilicates	20	1,210	4.5	100	14,583	BC
Fe oxides and hydrous oxides	29	550	2.5	122	2,656	C
Si oxides	8	7.1	2.6	1.5	33	D

Fig. 3. CDFs representing the log K_d (FQ) populations for humic substances (purple); 1:1 phyllosilicates (red); 1:2 non-swelling phyllosilicates (blue); 1:2 swelling phyllosilicates (green); Fe oxides and hydrous oxides (cyan); SiO_2 (black). Solid lines are result of fitting the data to Equation S11. N: total number of entries; GM: K_d (FQ) geometric mean [L kg^{-1}] (derived from 50th percentile of the fitted distributions); GSD: geometrical standard deviation; 5th and 95th indicate the 5th and 95th percentiles of the fitted distributions. Pearson coefficients were > 0.96 for all fittings. FLSD column indicates the statistical results of Fisher Least Significance Differences Test.

affinity for FQ compared to other soil components. Fe oxides and hydrous oxides showed a slightly lower geometric mean K_d (FQ) (~ 550 L kg^{-1}) than 1:1 and 1:2 phyllosilicates (~ 1000 – 2000 L kg^{-1}), suggesting a moderate sorption affinity for FQ. Contrarily, geometric mean K_d (FQ) values for both HS and 1:2 swelling phyllosilicates minerals were outstandingly high (~ 20,000 L kg^{-1}), confirming a strong sorption affinity for FQ in these soil phases. FLSD tests revealed statistically different K_d (FQ) populations for SiO_2 and Fe oxides, with this last being comparable to the K_d (FQ) population of 1:1 phyllosilicates. K_d (FQ) populations for 1:1 and 1:2 non-swelling phyllosilicates, as well as HS and 1:2 swelling phyllosilicates, were also comparable to each other.

4.2. Development and validation of a parametric model to predict K_d (FQ) in bulk soils

The calibration set for the K_d (FQ) prediction model in bulk soils consisted in the 222 K_d (FQ) entries compiled in the HS, Si, Fe and phyllosilicate fractions. Desorption processes were not considered in the model due to the low number of studies providing desorption information. We anticipated that besides the relative sorption affinity of each soil component, their relative abundance affects their final weight in the eventual overall K_d (FQ) in soils. Accordingly, K_d (FQ) may be expressed as the sum of the product of the K_d of each individual phase ($K_{d,phase\ i}$) and their respective fraction ($f_{phase\ i}$) in a bulk soil. For every soil pH, $K_{d,\ phase\ i}$ for HS and phyllosilicates could be calculated from normalized sorption coefficients (see Table 2) and pKa values representative of the target FQ (Eqs. 2 – 4), thus defining $K_{d,phase\ i}^{pH(FQ)}$. As normalized sorption coefficients for FQ species were not available for metal oxides and hydrous oxides, in order to include relevant oxides and hydrous oxides in soils (*i.e.*, Fe and Si) in the model, a pH-independent K_d (FQ) value of 7 and 550 L kg^{-1} were considered for Si ($K_{d,\ Si}$) and Fe ($K_{d,\ Fe}$) oxides and hydrous oxides, respectively, resulting from the geometric mean (*i.e.*, 50th percentile) calculated from each respective population (see Fig. 3), although K_d values at other percentiles could be also derived if required for risk assessment studies. Thus, K_d predictions were based on the relative contribution of HS, Fe oxides and hydrous oxides, SiO_2 and the three different phyllosilicates examined (*i.e.*, 1:1. 1:2 non-swelling and 1:2 swelling phyllosilicates), as K_d (FQ) data for other mineral components in soils that may be abundant (*e.g.*, calcite, dolomite, feldspar) were not available.

To estimate the relative fraction of the soil phases in a given bulk soil, a number of assumptions must be made (see Table S4). As HA and FA contents in soils are usually not reported, the fraction of HS in soils (f_{HS}) could be deduced using reported OM content as a surrogate property, with a correction factor of 0.317 to estimate HA and FA contents within the organic fraction and to exclude humin and other black carbon components (Ukalska-Jaruga et al., 2021). A factor of 2.0 was used to convert OC to OM when necessary (Pibryl, 2010). Assuming that clay minerals are mostly present within the clay fraction, the fraction of different phyllosilicates ($f_{PHYLLO,i}$) may be estimated, if necessary, from the reported clay content. Similarly, the SiO_2 fraction (f_{Si}) may be estimated using sand content as a surrogate property if quartz content is not provided. To account for the fraction of Fe oxides and hydrous oxides (f_{Fe}), only data on crystalline species derived from XRD was considered. All phase contents were referred to as bulk mass. The resulting model to estimate soil K_d (FQ) stands as Eq. 5:

$$K_d(FQ) = K_{d,HS}^{pH(FQ)} f_{HS} + K_{d,Si} f_{Si} + K_{d,Fe} f_{Fe} + \sum K_{d,PHYLLOi}^{pH(FQ)} f_{PHYLLOi} \tag{5}$$

The predictive performance of Eq. 5 was validated with data obtained in bulk soils, which were not considered during the calibration of the model (see Table S4). Within this soil validation set, the sum of fractions accounted by the examined phases range 20 – 94 % of the total soil mass. Fig. 4 displays predicted soil K_d (FQ), derived from Eq. 5, and the experimental soil K_d (FQ). A good prediction of the experimental data was achieved ($\log K_{d,model} = 1.0 (\pm 0.2) \log K_{d,experimental}$; $n = 68$), capturing 53 % of the data variance and with most of the K_d (FQ) predictions falling within ± 0.5 log units (see Fig. 4). Despite the partial percentage of the bulk soil described in some cases, the use of correction factors to estimate the contents of pure soil phases, the varying characterization methods to estimate soil pH, the limitations of Equation 1 to model K_d (FQ) at extreme pH values, and the feasible presence of organo-clay aggregates in bulk soil (humic substances coating of clay minerals may block sorption sites that are accounted in the model), Eq. 5 resulted successful to roughly estimate literature K_d (FQ) values in bulk soils. Examining individual contributions of organic and mineral components on the predicted K_d (FQ) confirmed a minor (< 2 %) contribution of both crystalline Si and Fe oxides and hydrous oxides in FQ sorption, even though for those soils with contents as high as 45 % w/w, and a predominant but varying contribution of HS and phyllosilicate minerals depending on their relative abundance in soil, with generally higher log K_d (FQ) values for soils containing swelling phyllosilicates (Fig. S6).

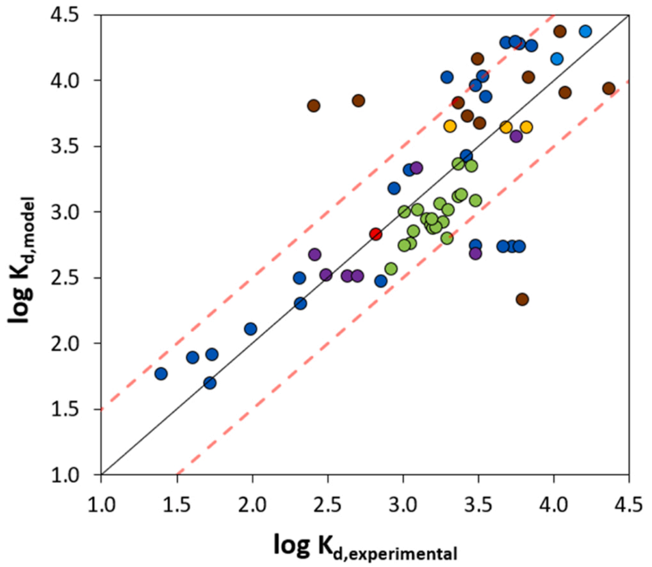

Fig. 4. K_d (FQ) prediction performance of Eq. 5 based on individual phase contributions for different K_d (FQ) experimental data in bulk soils (blue: Fabregat-Palau et al., 2022; purple: Nowara et al., 1997; green: Alvarez-Esmorís et al., 2022; red: Graouer-Bacart et al., 2015; cyan: Wu et al., 2014; brown: Zhou et al., 2014; orange: Riaz et al., 2019). Dashed red lines indicate ± 0.5 log K_d units uncertainty range.

To our knowledge, Eq. 5 stands as the first available parametric model to estimate K_d (FQ) in bulk soils that is based on the individual sorbing contributions of different soil phases and that is applicable to a wide range of FQ and soil properties. The inclusion of a pH-dependent normalized sorption coefficient ($K_{d,phase\ i}^{pH(FQ)}$) for different soil phases, being these derived from data compilations considering a variety of FQ and phase properties, allows a better assessment of the sorption features of different organic and mineral components at varying conditions.

5. Conclusions

The synthesis of K_d (FQ) datasets for humic substances, metal oxides, and phyllosilicate minerals allowed us to better elucidate the sorption mechanisms and main properties governing FQ sorption in these soil phases, and to predict their relative sorption contribution in bulk soils. A bell-shaped K_d (FQ) *vs.* pH pattern is observed for humic substances and phyllosilicate minerals, explaining around 50 % of the K_d (FQ) data variability and thus permitting the derivation of normalized sorption coefficients for each FQ species for each of these soil phases. Whereas sorption of FQ in phyllosilicates is mainly driven by cation exchange mechanisms, sorption in humic substances is governed by multiple interaction mechanisms depending on the tested pH, including hydrogen bond, electrostatic/cation exchange, cation-π, π-π and hydrophobic interactions. Metal oxides are capable of binding FQ through covalent FQ – metal bonds; at neutral pH, the FQ sorption sequence in metal oxides can be explained by the Irving-Langmuir series, whereas for a given metal oxide and pH, specific mineral properties (*i.e.*, SSA) govern K_d (FQ) variability. Statistical comparison of K_d (FQ) data populations for the different soil components permitted to rank their relative sorption affinity, and combined with their relative abundance in soils, set the basis for the development of a K_d (FQ) prediction model that was found successful to roughly predict K_d (FQ) data in bulk soils. Such an approach may also be applicable to other ionizable compounds with complex sorption in soils. Overall, this information may be useful for environmental modellers aiming to assess FQ interaction in soils based on specific interactions between FQ and different soil organic and mineral components.

CRediT authorship contribution statement

Peter Grathwohl: Writing – review & editing, Supervision. **Anna Rigol:** Writing – review & editing, Supervision, Resources, Project administration, Methodology, Funding acquisition, Conceptualization. **Joel Fabregat-Palau:** Writing – review & editing, Writing – original draft, Visualization, Validation, Methodology, Investigation, Formal analysis, Data curation, Conceptualization. **Miquel Vidal:** Writing – review & editing, Supervision, Resources, Project administration, Methodology, Funding acquisition, Conceptualization.

Declaration of Competing Interest

The authors declare that they have no known competing financial interests or personal relationships that could have appeared to influence the work reported in this paper.

Data Availability

Data will be made available on request.

Acknowledgements

This work was carried out in a Generalitat de Catalunya Research Group (2021 SGR 01342) and is part of the project PID2020–114551RB-I00 funded by MCIN/AEI/ 10.13039/501100011033. Joel Fabregat-Palau acknowledges support from the Open Access Publishing Fund of the University of Tübingen, and support of Amirhossein Ershadi and Binlong Liu for creating Fig. S4 and Fig. S6, respectively.

Appendix A. Supporting information

Supplementary data associated with this article can be found in the online version at doi:10.1016/j.ecoenv.2024.116535.

References

Alvarez-Esmorís, C., Rodríguez-López, L., Núñez-Delgado, A., Álvarez-Rodriguez, E., Fernández-Calviño, D., Arias-Estévez, M., 2022. Influence of pH on the adsorption-desorption of doxycycline, enrofloxacin, and sulfamethoxypyridazine in soils with var iable surface charge. Environ. Res. 214, 114071 https://doi.org/10.1016/j.envres.2022.114071.

Antilen, M., Bustos, O., Ramirez, G., Canales, C., Faundez, M., Escudey, M., Pizarro, C., 2016. Electrochemical evaluation of ciprofloxacin adsorption on soil organic matter. N. J. Chem. 40, 7132–7139. https://doi.org/10.1039/c6nj00207b.

Aristilde, L., Sposito, G., 2008. Molecular modeling of metal complexation by a fluoroquinolone antibiotic. Environ. Toxicol. Chem. 27 (11), 2304–2310. https://doi.org/10.1897/08-059.1.

Aristilde, L., Sposito, G., 2010. Binding of ciprofloxacin by humic substances: a molecular dynamics study. Environ. Toxicol. Chem. 29 (1), 90–98. https://doi.org/10.1002/etc.19.

Aristilde, L., Sposito, G., 2013. Complexes of the antimicrobial ciprofloxacin with soil, peat, and aquatic humic substances. Environ. Toxicol. Chem. 32 (7), 1467–1478. https://doi.org/10.1002/etc.2214.

Blanchard, G., Maunaye, M., Martin, G., 1984. Removal of heavy metals from waters by means of natural zeolites. Water Res. 18 (12), 1501–1507. https://doi.org/10.1016/0043-1354(84)90124-6.

Carmosini, N., Lee, L.S., 2009. Ciprofloxacin sorption by dissolved organic carbon from reference and bio-waste materials. Chemosphere 77 (6), 813–820. https://doi.org/10.1016/j.chemosphere.2009.08.003.

Chang, P.H., Jiang, W.T., Li, Z., Kuo, C.Y., Wu, Q., Jean, J.S., Lv, G., 2016. Interaction of ciprofloxacin and probe compounds with palygorskite PFl-1. J. Hazard. Mater. 303, 55–63. https://doi.org/10.1016/j.jhazmat.2015.10.012.

Chen, G., Liu, X., Tartakevosky, D., Li, M., 2016. Risk assessment of three fluoroquinolone antibiotics in the groundwater recharge system. Ecotoxicol. Environ. Saf. 133, 18–24. https://doi.org/10.1016/j.ecoenv.2016.05.030.

Chen, J., Xu, Y., Zheng, D., Wei, Q., Farooq, U., Lu, T., Chen, W., Qi, Z., 2022. The mechanisms involved into the inhibitory effects of ionic liquids chemistry on adsorption performance of ciprofloxacin onto inorganic minerals. Colloids Surf. A 648, 129422. https://doi.org/10.1016/j.colsurfa.2022.129422.

Cheng, W., Hanna, K., 2018. Influence of magnetite stoichiometry on the binding of emerging organic contaminants, 2018 Environ. Sci. Technol. 52 (2), 467–473. https://doi.org/10.1021/acs.est.7b04849.

Conkle, J.L., Lattao, C., White, J.R., Cook, R.L., 2010. Competitive sorption and desorption behavior for three fluoroquinolone antibiotics in a wastewater treatment wetland soil. Chemosphere 80 (11), 1353–1359. https://doi.org/10.1016/j.chemosphere.2010.06.012.

Cuprys, A., Pulicharla, R., Kaur Brar, S., Drogui, P., Verma, M., Surampalli, R.Y., 2018. Fluoroquinolones metal complexation and its environmental impacts. Coord. Chem. Rev. 376, 46–61. https://doi.org/10.1016/j.ccr.2018.05.019.

Ding, F., Li, Y., He, T., Ou, D., Huang, Y., Yin, G., Yang, J., Wu, S., He, E., Liu, M., 2024. Urban agglomerations as an environmental dimension of antibiotics transmission through the "One Health" lens. J. Hazard. Mat. 465, 133283 https://doi.org/10.1016/j.jhazmat.2023.133283.

Du, J., Zhao, H., Wang, Y., Xie, H., Zhu, M., Chen, J., 2019. Presence and environmental risk assessment of selected antibiotics in coastal water adjacent to mariculture areas in the Bohai Sea. Ecotox. Environ. Saf. 177, 117–123. https://doi.org/10.1016/j.ecoenv.2019.03.075.

EMA, 2019. European Medicines Agency, Science Medicines Health. EMA/175398/2019. ⟨https://www.ema.europa.eu/en/documents/referral/quinolone-fluoroquinolone-article-31-referral-disabling-potentially-permanent-side-effects-lead_en.pdf⟩. Accsessed 27th Jan. 2024.

Fabregat-Palau, J., Yu, Z., Zeng, X., Vidal, M., Rigol, A., 2022. Deriving parametric and probabilistic K_d values for fluoroquinolones in soils. Sci. Total Environ. 861, 160266 https://doi.org/10.1016/j.scitotenv.2022.160266.

Fabregat-Palau, J., Rigol, A., Yu, Z., Vidal, M., 2023. Using a batch test to derive sorption data of fluoroquinolones in humic acids. Methods X 10, 102109. https://doi.org/10.1016/j.mex.2023.102109.

Fang, L., Chen, C., Li, S.-Y., Ye, P., Shi, Y., Sharma, G., Sakar, B., Shaheen, S., Lee, S.-S., Xiao, R., Chen, X., 2023. A comprehensive and global evaluation of residual antibiotics in agricultural soils: accumulation, potential ecological risks, and attenuation strategies. Ecotoxicol. Environ. Saf. 262, 115175 https://doi.org/10.1016/j.ecoenv.2023.115175.

Fries, E., Crouzet, C., Michel, C., Togola, A., 2016. Interactions of ciprofloxacin (CIP), titanium dioxide (TiO2) nanoparticles and natural organic matter (NOM) in aqueous suspensions. Sci. Total Environ. 563 – 564, 971–976. https://doi.org/10.1016/j.scitotenv.2015.12.023.

Gan, Y., Wei, Y., Xiong, J., Cheng, G., 2018. Impact of post-processing modes of precursor on adsorption and photocatalytic capability of mesoporous TiO2 nanocrystallite aggregates towards ciprofloxacin removal. Chem. Eng. J. 349, 1–16. https://doi.org/10.1016/j.cej.2018.05.051.

Gong, W., Liu, X., He, H., Wang, L., Dai, G., 2012. Quantitatively modeling soil-water distribution coefficients of three antibiotics using soil physicochemical properties. Chemosphere 89 (7), 825–831. https://doi.org/10.1016/j.chemosphere.2012.04.064.

Goyne, K.W., Chorover, J., Kubicki, J.D., Zimmerman, A.R., Brantley, S.L., 2005. Sorption of the antibiotic ofloxacin to mesoporous and nonporous alumina and silica. J. Colloid Interface Sci. 283 (1), 160–170. https://doi.org/10.1016/j.jcis.2004.08.150.

Graouer-Bacart, M., Sayen, S., Guillin, E., 2015. Adsorption of enrofloxacin in presence of Zn (II) on a calcareous soil. Ecotoxicol. Environ. Saf. 122, 470–476. https://doi.org/10.1016/j.ecoenv.2015.09.019.

Gu, C., Karthikeyan, K.G., 2005. Sorption of the antimicrobial ciprofloxacin to aluminum and iron hydrous oxides. Environ. Sci. Technol. 39 (23), 9166–9173. https://doi.org/10.1021/es051109f.

Hanamoto, S., Ogawa, F., 2019. Predicting the sorption of azithromycin and levofloxacin to sediments from mineral and organic components. Environ. Pollut. 255, 113180 https://doi.org/10.1016/j.envpol.2019.113180.

Irving, H., Williams, R.J.P., 1953. The stability of transition metal complexes. J. Chem. Soc. 637, 3192–3210. https://doi.org/10.1016/j.jes.2018.04.016.

Jacobson, A.T., Fan, M., 2019. Evaluation of natural goethite on the removal of arsenate and selenite from water. J. Environ. Sci. 76, 133–141. https://doi.org/10.1016/j.jes.2018.04.016.

Leal, R.M.P., Alleoni, L.R.F., Tornisielo, V.L., Regitano, J.B., 2013. Sorption of fluoroquinolones and sulfonamides in 13 Brazilian soils. Chemosphere 92 (8), 979–985. https://doi.org/10.1016/j.chemosphere.2013.03.018.

Li, X., Bi, E., 2019. Different surface complexation patterns of gatifloxacin at typical iron mineral/water interfaces. Environ. Earth Sci. 78, 630. https://doi.org/10.1007/s12665-019-8641-1.

Li, Y., Bi, E., Chen, H., 2017. Sorption Behavior of Ofloxacin to Kaolinite: effects of pH, ionic strength, and Cu(II). Water Air Soil Pollut. 228 (46), 1–10. https://doi.org/10.1007/s11270-016-3236-x.

Li, Y., Bi, E., Chen, H., 2019. Effects of dissolved humic acid on fluoroquinolones sorption and retention to kaolinite. Ecotoxicol. Environ. Saf. 178, 43–50. https://doi.org/10.1016/j.ecoenv.2019.04.002.

Li, Z., Hong, H., Liao, L., Ackley, C.J., Schulz, L.A., Macdonald, R.A., Mihelich, A.L., Emard, S.M., 2011. A mechanistic study of ciprofloxacin removal by kaolinite. Colloids Surf. B 88 (1), 339–344. https://doi.org/10.1016/j.colsurfb.2011.07.011.

Liu, S., Wu, P., Yu, L., Li, L., Gong, B., Zhu, N., Dang, Z., Yang, C., 2017. Preparation and characterization of organo-vermiculite based on phosphatidylcholine and adsorption of two typical antibiotics. Appl. Clay Sci. 137, 160–167. https://doi.org/10.1016/j.clay.2016.12.002.

Liu, X., Lu, S., Liu, Y., Meng, W., Zheng, B., 2017. Adsorption of sulfamethoxazole (SMZ) and ciprofloxacin (CIP) by humic acid (HA): characteristics and mechanism. RSC Adv. 7 (80), 50449–50458. https://doi.org/10.1039/C7RA06231A.

Lorphensri, O., Intravijit, J., Sabatini, D.A., Kibbey, T.C.G., Osathaphan, K., Saiwan, C., 2006. Sorption of acetaminophen, 17α-ethynyl estradiol, nalidixic acid, and norfloxacin to silica, alumina, and a hydrophobic medium. Water Res. 40 (7), 1481–1491. https://doi.org/10.1016/j.watres.2006.02.003.

Lützhøft, H.C.H., Vaes, W.H.J., Freidig, A.P., Halling-Sørensen, B., Hermens, J.L.M., 2000. Influence of pH and other modifying factors on the distribution behavior of 4-quinolones to solid phases and humic acids studied by "negligible-depletion" SPME-HPLC. Environ. Sci. Technol. 34 (23), 4989–4994. https://doi.org/10.1021/es000917y.

Lv, G., Pearce, C.W., Gleason, A., Liao, L., Macwilliams, M.P., Li, Z., 2013. Influence of montmorillonite on antimicrobial activity of tetracycline and ciprofloxacin. J. Asian Earth Sci. 77, 281–286. https://doi.org/10.1016/j.jseaes.2013.04.025.

Martin, S., Shchukarev, A., Hanna, K., Boily, J.F., 2015. Kinetics and mechanisms of Ciprofloxacin oxidation on hematite surfaces. Environ. Sci. Technol. 49 (20), 12197–12205. https://doi.org/10.1021/acs.est.5b02851.

Martínez-Mejía, M.J., Sato, I., Rath, S., 2017. Sorption mechanism of enrofloxacin on humic acids extracted from Brazilian soils. Environ. Sci. Pollut. Res. 24 (19), 15995–16006. https://doi.org/10.1007/s11356-017-9210-3.

Moradi, S.E., Haji Shabani, A.M., Dadfarnia, S., Emami, S., 2016. Effective removal of ciprofloxacin from aqueous solutions using magnetic metal–organic framework sorbents: mechanisms, isotherms and kinetics. J. Iran. Chem. Soc. 13 (9), 1617–1627. https://doi.org/10.1007/s13738-016-0878-y.

Najafpoor, A.A., Nemati Sani, O., Alidadi, H., Yazdani, M., Navaei Fezabady, A.A., Taghavi, M., 2019. Optimization of ciprofloxacin adsorption from synthetic wastewaters using γ-Al2O3 nanoparticles: an experimental design based on response surface methodology. Colloids Inter. Sci. Comm. 33, 100212 https://doi.org/10.1016/j.colcom.2019.100212.

Nowara, A., Burhenne, J., Spiteller, M., 1997. Binding of fluoroquinolone carboxylic acid derivatives to clay minerals. J. Agric. Food Chem. 45 (4), 1459–1463. https://doi.org/10.1021/jf960215l.

OECD, 2000. OECD 106 Adsorption - Desorption Using a Batch Equilibrium Method. OECD Guideline for the Testing of Chemicals. 〈https://doi.org/10.1787/9789264069602-en〉.

Okaikue-Woodi, F.E.K., Kelch, S.E., Schmidt, M.P., Martinez, C.E., Youngman, R.E., Aristide, L., 2018. Structures and mechanisms in clay nanopore trapping of structurally-different fluoroquinolone antimicrobials. J. Colloid Inter. Sci. 513, 367–378. https://doi.org/10.1016/j.jcis.2017.11.020.

Pan, B., Wang, P., Wu, M., Li, J., Zhang, D., Xiao, D., 2012b. Sorption kinetics of ofloxacin in soils and mineral particles. Environ. Pollut. 171, 185–190. https://doi.org/10.1016/j.envpol.2012.07.037.

Pan, B., Qiu, M., Wu, M., Zhang, D., Peng, H., Wu, D., Xing, B., 2012a. The opposite impacts of Cu and Mg cations on dissolved organic matter-ofloxacin interaction. Environ. Pollut. 161, 76–82. https://doi.org/10.1016/j.envpol.2011.09.040.

Paul, T., MacHesky, M.L., Strathmann, T.J., 2012. Surface complexation of the zwitterionic fluoroquinolone antibiotic ofloxacin to nano-anatase TiO2 photocatalyst surfaces. Environ. Sci. Technol. 46 (21), 11896–11904. https://doi.org/10.1021/es302097k.

Paul, T., Liu, J., Machesky, M.L., Strathmann, T.J., 2014. Adsorption of zwitterionic fluoroquinolone antibacterials to goethite: a charge distribution-multisite complexation model. J. Colloid Interface Sci. 428, 63–72. https://doi.org/10.1016/j.jcis.2014.04.034.

Pei, Z., Shan, X.Q., Kong, J., Wen, B., Owens, G., 2010. Coadsorption of ciprofloxacin and Cu(II) on montmorillonite and kaolinite as affected by solution pH. Environ. Sci. Technol. 44 (3), 915–920. https://doi.org/10.1021/es902902c.

Pei, Z.G., Shan, X.Q., Zhang, S.Z., Kong, J.J., Wen, B., Zhang, J., Zheng, L.R., Xie, Y.N., Janssens, K., 2011. Insight to ternary complexes of co-adsorption of norfloxacin and Cu(II) onto montmorillonite at different pH using EXAFS. J. Hazard. Mater. 186 (1), 842–848. https://doi.org/10.1016/j.jhazmat.2010.11.076.

Peruchi, L.M., Fostier, A.H., Rath, S., 2015. Sorption of norfloxacin in soils: analytical method, kinetics and Freundlich isotherms. Chemosphere 119, 310–317. https://doi.org/10.1016/j.chemosphere.2014.06.008.

Pibryl, 2010. A critical review of the conventional SOC to SOM conversion factor. Geoderma 156 (3-4), 75–83. https://doi.org/10.1016/j.geoderma.2010.02.003.

Qin, X., Liu, F., Wang, G., Weng, L., Li, L., 2014. Adsorption of levofloxacin onto goethite: effects of pH, calcium and phosphate. Colloids Surf. B 116, 591–596. https://doi.org/10.1016/j.colsurfb.2013.09.056.

Rakshit, S., Sarkar, D., Elzinga, E.J., Punamiya, P., Datta, R., 2013. Mechanisms of ciprofloxacin removal by nano-sized magnetite. J. Hazard. Mater. 246 – 247, 221–226. https://doi.org/10.1016/j.jhazmat.2012.12.032.

Ramírez-Guinart, O., Kaplan, D., Rigol, A., Vidal, M., 2022. Deriving probabilistic soil distribution coefficients (Kd). Part 1: general approach to decreasing and descriving variability and example using uranium Kd values. J. Environ. Radioac. 222, 106362 https://doi.org/10.1016/j.envrad.2020.106362.

Redgrave, L.S., Sutton, S.B., Webber, M.A., Piddock, L.J.V., 2014. Fluoroquinolone resistance: mechanisms, impact on bacteria, and role in evolutionary success. Trends Microbiol. 22 (8), 438–445. https://doi.org/10.1016/j.tim.2014.04.007.

Riaz, L., Mahmood, T., Khalid, A., Rashid, A., Ahmed Siddique, M.B., Kamal, A., Coyne, M.S., 2018. Fluoroquinolones (FQs) in the environment: a review on their abundance, sorption and toxicity in soil. Chemosphere 191, 704–720. https://doi.org/10.1016/j.chemosphere.2017.10.092.

Riaz, L., Mahmood, T., Qingxiang, Y., Yasir, M.W., Rashid, A., Coyn, M.S., D'angelo, E., 2019. Sorption and desorption behavior of fluoroquinolone antibiotics in an agricultural soil. Pedosphere 29 (5), 676–680. https://doi.org/10.1016/S1002-0160(19)60831-3.

Rivagli, E., Pastorello, A., Sturini, M., Maraschi, F., Speltini, A., Zampori, L., Setti, M., Malavasi, L., Profumo, A., 2014. Clay minerals for adsorption of veterinary FQs: behavior and modeling. J. Environ. Chem. Eng. 2 (1), 738–744. https://doi.org/10.1016/j.jece.2013.11.017.

Roca, M.E., Baschini, M., Sapag, K., 2015. Influence of pH and antibiotic solubility on the removal of ciprofloxacin from aqueous media using montmorillonite. Appl. Clay Sci. 114, 69–76. https://doi.org/10.1016/j.clay.2015.05.010.

Schmitt-Kopplin, P., Burhenne, J., Freitag, D., Spiteller, M., Kettrup, A., 1999. Development of capillary electrophopresis methods for the analysis of fluoroquinolones and application to the study of the influence of humic substances on their photodegradation in aqueous phase. J. Chromatogr. A 837 (1-2), 253–265. https://doi.org/10.1016/S0021-9673(99)00079-5.

Septian, A., Oh, S., Shin, W.S., 2018. Sorption of antibiotics onto montmorillonite and kaolinite: competition modelling. Environ. Technol. 40 (22), 1–14. https://doi.org/10.1080/09593330.2018.1459870.

Shao, S., Pan, W., Wang, B., Liu, Y., Gan, H., Li, M., Liao, T., Yang, X., Yang, Q., Huang, C., Geng, M., Pan, G., Liu, K., Zhu, P., Tao, F., 2023. Association between antibiotic exposure and the risk of infertility in women of childbearing age: a case-control study. Ecotoxicol. Envion. Saf. 249, 114414 https://doi.org/10.1016/j.ecoen.2022.114414.

Singaraj, S.G., Mahanty, B., Balachandran, D., Padmaprabha, A., 2019. Adsorption and desorption of chromium with humic acid coated iron oxide nanoparticles. Environ. Sci. Pollut. R. 26, 30044–30054. https://doi.org/10.1007/s11356-019-06164-0.

Tan, Y., Guo, Y., Gu, X., Gu, C., 2015. Effects of metal Cations and Fulvic acid on the adsorption of ciprofloxacin onto goethite. Environ. Sci. Pollut. Res. 22 (1), 609–617. https://doi.org/10.1007/s11356-014-3351-4.

Teixidó, M., Pignatello, J.J., Beltrán, J.L., Granados, M., Peccia, J., 2011. Speciation of the ionizable antibiotic sulfamethazine on black carbon (Biochar). Environ. Sci. Technol. 45 (23), 10020–10027. https://doi.org/10.1021/es202487h.

Trivedi, P., Vasudevan, D., 2007. Spectroscopic investigation of ciprofloxacin speciation at the goethite-water interface. Environ. Sci. Technol. 41 (9), 3153–3158. https://doi.org/10.1021/es061921y.

Ukalska-Jaruga, A., Bejger, R., Debaene, G., Smreczak, B., 2021. Characterization of soil organic matter individual fractions (fulvic acids, humic acids and humin) by spectroscopic and electrochemical techniques in agricultural soils. Agronomy 11 (6), 1067. https://doi.org/10.3390/agronomy11061067.

USEPA, 2007. Foundations and Frameworks for Human Microbial Risk Assessment. Center for Risk Science and Public Health School of Public Health and Health Services, The George Washinton University Medical Center, Washinton DC. U.S. Environmental Protection Agency.

USEPA, 2009. Guidance on the Development, Evaluation, and Application of Environmental Models. U.S. Environmental Protection Agency. EPA/100/K-09/003. papers2://publication/uuid/06FC4BA9-AC^{3}B–^{4}E49-A54F-950F3200B970.

Van, T.T.H., Yidana, Z., Smooker, P.M., Coloe, P.J., 2020. Antibiotic use in food animals worldwide, with a focus on Africa: pluses and minuses. J. Glob. Antimicrob. Resist. 20, 170–177. https://doi.org/10.1016/j.jgar.2019.07.031.

Van Doorslaer, X., Dewulf, J., Van Langenhove, H., Demeestere, K., 2014. Fluoroquinolone antibiotics: an emerging class of environmental micropollutants. Sci. Total Environ. 500 – 501, 250–269. https://doi.org/10.1016/j.scitotenv.2014.08.075.

Vasudevan, D., Bruland, G.L., Torrance, B.S., Upchurch, V.G., Mackay, A.A., 2009. pH-dependent ciprofloxacin sorption to soils: interaction mechanisms and soil factors influencing sorption. Geoderma 151, 68–76. https://doi.org/10.1016/j.geoderma.2009.03.007.

Wan, M., Li, Z., Hong, H., Wu, Q., 2013. Enrofloxacin uptake and retention on different types of clays. J. Asian Earth Sci. 77, 287–294. https://doi.org/10.1016/j.jseaes.2013.02.032.

Wang, C., Ma, L., Liu, B., Zhang, D., Pan, B., 2017. Co-contaminant effects on ofloxacin adsorption onto activated carbon, graphite, and humic acid. Environ. Sci. Pollut. Res. 24, 23834–23842. https://doi.org/10.1007/s11356-017-0038-7.

Wang, C.J., Li, Z., Jiang, W.T., 2011. Adsorption of ciprofloxacin on 2:1 dioctahedral clay minerals. Appl. Clay Sci. 53 (4), 723–728. https://doi.org/10.1016/j.clay.2011.06.014.

Wang, L., Liang, N., Li, H., Yang, Y., Zhang, D., Liao, S., Pan, B., 2015. Quantifying the dynamic fluorescence quenching of phenanthrene and ofloxacin by dissolved humic acids. Environ. Pollut. 196, 379–385. https://doi.org/10.1016/j.envpol.2014.10.029.

Wang, L., Zhang, L., Feng, B., Hua, X., Li, Y., Zhang, W., Guo, Z., 2022. The pH dependence and role of fluorinated substituent of enoxacin binding to ferrihydrite. Sci. Total Environ. 823, 153707 https://doi.org/10.1016/j.scitotenv.2022.153707.

WHO, 2017. Global Priority list of antibiotic-resistance bacteria to guide research, discovery, and development of new antibiotics. World Health Organization, Geneva. J. Med. Soc. 32 (1), 76–77. https://doi.org/10.4103/jms.jms_25_17.

Wu, D., Li, H., Liao, S., Sun, X., Peng, H., Zhang, D., Pan, B., 2014. Co-sorption of ofloxacin and Cu(II) in soils before and after organic matter removal. Sci. Total Environ. 481, 209–216. https://doi.org/10.1016/j.scitotenv.2014.02.041.

Wu, Q., Li, Z., Hong, H., Yin, K., Tie, L., 2010. Adsorption and intercation of ciprofloxacin on montmorillonite. Appl. Clay Sci. 50, 204–211. https://doi.org/10.1016/j.clay.2010.08.001.

Wu, Q., Li, Z., Hong, H., 2012b. Influence of types and charges of exchangable cations on Ciprofloxacin sorption by Montmorillonite. J. Wuhan. Univ. Technol. Mater. Sci. Ed. 27 (3), 516–522. https://doi.org/10.1007/s11595-012-0495-2.

Wu, Q., Li, Z., Hong, H., Li, R., Jiang, W., 2012a. Desorption of ciprofloxacin from clay mineral surfaces. Water Res. 47 (1), 259–268. https://doi.org/10.1016/j.watres.2012.10.010.

Yan, W., Hu, S., Jing, C., 2012. Enrofloxacin sorption on smectite clays: effects of pH, cations, and humic acid. J. Colloid Interface Sci. 372 (1), 141–147. https://doi.org/10.1016/j.jcis.2012.01.016.

Yao, L., Li, Y., Li, Z., Shen, D., Feng, H., Zhou, H., Wang, M., 2020. Prevalence of fluoroquinolone, macrolide and sulfonamide-related resistance genes in landfills from East China, mainly driven by MGEs. Ecotoxicol. Environ. Saf. 190, 110131 https://doi.org/10.1016/j.ecoenv.2019.110131.

Zhang, H., Huang, C.H., 2007. Adsorption and oxidation of fluoroquinolone antibacterial agents and structurally related amines with goethite. Chemosphere 66 (8), 1502–1512. https://doi.org/10.1016/j.chemosphere.2006.08.024.

Zhang, J., Liu, Z., Song, S., Fang, J., Wang, L., Zhao, L., Li, C., Li, W., Byun, H.-M., Guo, L., Li, P., 2022. The exposure levels and health risk assessment of antibiotics in urine and its association with platelet mitochondrial DNA methylation in adults from Tianjin, China: a preliminary study. Ecotoxicol. Enviorn. Saf. 231, 113204 https://doi.org/10.1016/j.ecoen.2022.113204.

Zhang, Q., Zhao, L., Dong, Y.H., Huang, G.Y., 2012. Sorption of norfloxacin onto humic acid extracted from weathered coal. J. Environ. Manag. 102, 165–172. https://doi.org/10.1016/j.jenvman.2011.12.036.

Zhao, L., Liu, J., Wang, H., Dong, Y.H., 2019. Sorption of copper and norfloxacin onto humic acid: effects of pH, ionic strength, and foreign ions. Environ. Sci. Pollut. Res. 26 (11), 10685–10694. https://doi.org/10.1007/s11356-019-04515-5.

Zhao, Q., Zhang, S., Zhang, X., Lei, L., Ma, W., Ma, C., Song, L., 2017. Cation–Pi Interaction: a Key force for sorption of fluoroquinolone antibiotics on pyrogenic carbonaceous materials. Environ. Sci. Technol. 51 (23), 13659–13667. https://doi.org/10.1021/acs.est.7b02317.

Zhao, X., Hu, Z., Yang, X., Cai, X., Wang, Z., Xie, X., 2019. Noncovalent interactions between fluoroquinolone antibiotics with dissolved organic matter: a 1H NMR binding site study and multi-spectroscopic methods. Environ. Pollut. 248, 815–822. https://doi.org/10.1016/j.envpol.2019.02.077.

Zhou, D., Chen, B., Wu, M., Liang, N., Zhang, D., Li, H., Pan, B., 2014. Ofloxacin sorption in soils after long-term tillage: the contribution of organic and mineral compositions. Sci. Total Environ. 497 – 498, 665–670. https://doi.org/10.1016/j.scitotenv.2014.07.130.

Zhu, Y., Yang, K., Shan, R., Han, Z., Shao, Y., Tian, C., 2018. The Influence of Humification Degree of Humic Acid on Its Sorption of Norfloxacin during sewage sludge composting. Water Air Soil Pollut. 229 (5) https://doi.org/10.1007/s11270-018-3821-2.

Zhu, Y., Yang, Q., Lu, T., Qi, W., Zhang, H., Wang, M., Qi, Z., Chen, W., 2020. Effect of phosphate on the adsorption of antibiotics onto iron oxide minerals: comparison between tetracycline and ciprofloxacin. Ecotox. Environ. Saf. 205, 111345 https://doi.org/10.1016/j.ecoenv.2020.111345.